T-type NPC Inverter with Active Power Decoupling Method using Discontinuous Current Mode for Micro-Inverter

Akiyoshi Omomo, Jun-ichi Itoh, Keisuke Kusaka, Nagisa Takaoka, Hoai Nam Le
*Nagaoka University of Technology
Nagaoka, Niigata, Japan
itoh@vos.nagaokaut.ac.jp

***Abstract*—This paper presents a power decoupling control method for a T-type NPC inverter with a discontinuous current mode (DCM). The proposed method does not require additional components for active power decoupling method. Furthermore, the grid-tied inductor is minimized because the output current of the inverter is in DCM. The operation of the proposed method is confirmed with a prototype. Consequently, the second order harmonic component of the input current is reduced by 67.7% compared to that without the power decoupling control, whereas the output current THD is 1.9% at an output power of 500 W.**

Keywords—Micro inverter; PV system; Active power decoupling; Discontinuous current mode.

I. INTRODUCTION

Solar energy is attracting the attention as one of the dominant renewable energy sources [1–5]. In recent years, micro inverters are actively employed for photovoltaic systems in order to ensure maximal power from photovoltaic panels [6–10]. When the micro inverters are connected to AC grids, a power decoupling capability is required in the DC side. The reason is that there is an instantaneous power difference between the input and the output of a DC-AC inverter. In order to suppress the power ripple, in general, large electrolytic capacitors are installed to absorb the power ripple at double line frequency. However, the electrolytic capacitors have high losses due to their high ESR, suffer from short life time compared with film capacitors [11].

As the power decoupling method, the power decoupling controls with an additional circuit using film or ceramic capacitors, inductors and switching devices, have been already proposed [12–14]. System life time becomes longer by employing ceramic or film capacitors instead of the electrolytic capacitors. However, its cost and weight increase because of the additional circuit for power decoupling control.

In order to avoid applying additional components, the power decoupling method for single phase T-type NPC inverter is proposed [15]. This method simultaneously achieves an output current control and a power decoupling control despite one inductor. Note that the current for achieving power decoupling control is defined as “neutral point current” in this paper because the power decoupling control is achieved by flowing the current through the neutral point in the T-type NPC inverter. In the conventional method, Continuous Current Mode (CCM) is applied for the current control method. In general, one inductor is required for one current control in CCM. On the other hands, the circuit has only one inductor. Thus, there are the terms that the output current control and neutral point current control interrupt each other. The term is named “current uncontrollable period” in this paper.

In this paper, the active power decoupling method for single phase T-type NPC inverter in order to eliminate the current control interruption. As the feature of the proposed method, DCM is applied for the current control method instead of CCM in order to avoid the current control interruption without additional inductors. Moreover, the output side inductor is minimized by applying DCM. The advantage of the proposed method is that both elimination of the electrolytic capacitors and the minimization of the system can be simultaneously achieved. This paper is organized as follows; first, the principle of the active power decoupling method is explained, second, the circuit configuration and the conventional active power decoupling control for T-type NPC inverter is explained. Third, the proposed active power decoupling control based on DCM is introduced. Finally, the operation of the proposed method is confirmed in the simulation and the experiment at an output power of 500 W.

II. PRINCIPLE OF ACTIVE POWER DECOUPLING METHOD

In this section, the principle of an occurring power ripple in a DC-AC circuit and absorbing the power ripple by a decoupling control is explained. The output voltage and the output current of an inverter are respectively represented as

$$v_{out} = \sqrt{2}V_{out}\sin\left(\omega t\right) \quad (1),$$

$$i_{out} = \sqrt{2}I_{out}\sin\left(\omega t\right) \quad (2),$$

where the capital letter indicates the RMS value of their instantaneous value, and ω is the grid angular frequency. Thus, the instantaneous output power is represented as

$$\begin{aligned} p_{out} &= v_{out}i_{out} = V_{out}I_{out} - V_{out}I_{out}\cos(2\omega t) \\ &= P_{Active} + p_{\mathrm{Re}active} \end{aligned} \quad (3),$$

where P_{Active} is the active power which is a constant value and p_{Reacct} is the reactive power, which is fluctuation value. Eq. 3 indicates that a power ripple at twice the grid frequency is occurred in an inverter whereas the input power is constant.

Figure 1 shows the relationship among the input power, the output power, and the compensation power in the buffer capacitor. From Fig. 1, the output power oscillates at twice the grid frequency, whereas the input power should be constant. In order to compensate the power ripple, the instantaneous power difference between the input and the output is compensated by charging and discharging the buffer capacitor according to $p_{Reactive}$ in Eq. 3 as shown in Fig. 1(b). The relationship of the $p_{Reactive}$ and the charged and discharged energy of the buffer capacitor is represented as

$$\Delta E = \frac{1}{2} C\left(V_{\max}{}^{2} - V_{\min}{}^{2}\right) \quad (4),$$

where ΔE is the buffer energy, which is the decoupling capability of the buffer capacitor, C is the capacitance, V_{max} is the maximum and V_{min} is the minimum value of the oscillated voltage of the buffer capacitor. As shown in Eq. 4, the compensation energy is dependent to the capacitance and the voltage ripple of the capacitor. In general, bulky electrolytic capacitors are used at the DC-Link stage in DC-AC converter in order to absorb the power ripple.

However, in the active power decoupling method, additional switching devices, inductors, small capacitors are employed for the active buffer circuit instead of applying bulky electrolytic capacitors in the DC-link [12–14]. The buffer capacitor voltage is oscillated by controlling the current on the inductor in the power decoupling circuit. As a result, the buffer capacitor absorbs the same power ripple with a small capacitance due to the increase of voltage ripple $V_{max}{}^{2}$-$V_{min}{}^{2}$ in Eq. 4. Therefore, a film or ceramic capacitors can be used instead of the electrolytic capacitor to increase the lifetime of the system.

III. Circuit Configuration and Proposed Active Power Decoupling Mehotd

Figure 2 shows the circuit configuration of the single-phase T-type NPC inverter. In T-type NPC inverter, the power flow is bidirectional. In this paper, the power flow is defined from the DC side to the AC side. In the conventional method in [14], the active power decoupling control is achieved by the oscillation of the two capacitor voltages V_{C1} and V_{C2} in opposite phase.

Figure 3 shows the ideal waveforms of the two capacitor voltages and the summation of the two capacitor voltages which is DC-Link voltage. The two capacitor voltages V_{C1} and V_{C2} are represented as

$$V_{C1} = \frac{V_{dc}}{2} + V_m \sin(\omega t + \delta) \quad (5),$$

$$V_{C2} = \frac{V_{dc}}{2} - V_m \sin(\omega t + \delta) \quad (6),$$

where V_{dc} is the DC-link voltage, V_m is an amplitude of the two of capacitor voltages, ω is the angular grid frequency, and δ is the initial phase against the output voltage. As shown in Fig. 3

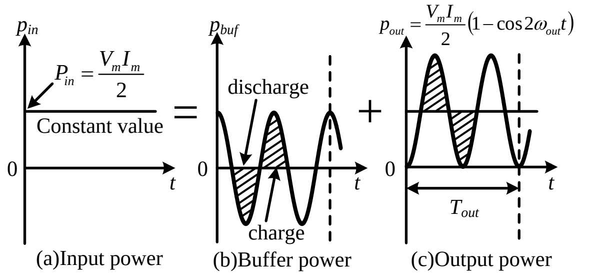

Fig. 1. Principal of power ripple compensation in Single-phase DC-AC converter.

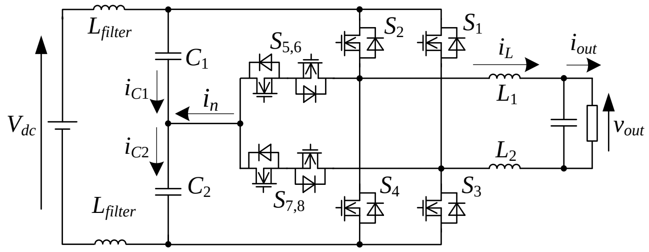

Fig. 2. Single phase T-type NPC inverter. The output current control and neutral point current are controlled by only one series of inducotor L_1 and L_2

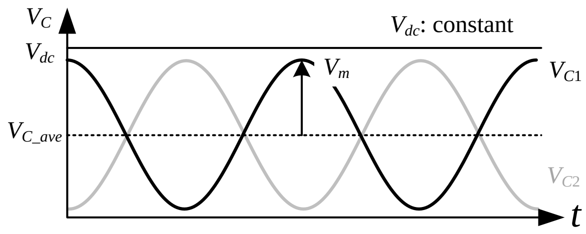

Fig. 3. Waveforms of ideal capacitor voltages and the summation of the two capacitor voltages which is DC-link voltage. The two capacitor voltages are oscillated in opposite phase.

and Eqs. (5–6), the DC-link voltage is the summation of the two capacitor voltages, which is constant, because the power decoupling control is achieved by oscillating the two capacitor voltages in opposite phases. From Eqs. (5–6), the capacitor currents i_{C1} and i_{C2} are given by

$$i_{C1} = C\frac{dV_{C1}}{dt} = C\omega V_m \cos(\omega t + \delta) \quad (7),$$

$$i_{C2} = C\frac{dV_{C2}}{dt} = -C\omega V_m \cos(\omega t + \delta) \quad (8),$$

where C is the capacitance of the two of DC-Link capacitors C_1 and C_2. The neutral point current is calculated as

$$i_n = i_{C1} - i_{C2} = 2C\omega V_m \cos(\omega t + \delta) \quad (9),$$

From Eqs. (5–9), capacitor voltages are controlled by the neutral point current. In addition, from Eqs. (5–8), the instantaneous capacitor power is given by

$$p_C = C\omega V_m{}^{2} \sin(\omega t + \delta)\cos(\omega t + \delta)$$
$$= \frac{1}{2} C\omega V_m{}^{2} \sin(2\omega t + 2\delta) \quad (10).$$

In order to absorb the power ripple, Eq. 10 has to be same as $p_{Reacitve}$ in Eq. 3. In Eq. 10 and $p_{Reactive}$ in Eq. 3, the variation is only sinusoidal function term. Thus, the constant value and the variation are respectively compared. The constant value, which means amplitude, and the variation, which means phase, are respectively compared in Eqs. (11–12)

$$-\cos(2\omega t) = \sin(2\omega t + 2\delta) \qquad (11)$$

$$V_{out} I_{out} = C\omega V_m^{\ 2} \qquad (12).$$

From Eq. 11, the initial phase difference of the neutral point current δ is calculated. Moreover, from Eq. 12, the amplitude of the capacitor voltage V_m is determined. Then, V_m is represented as

$$V_m = \sqrt{\frac{V_{out} I_{out}}{C\omega}} \qquad (13).$$

Note that V_m should not exceed the half of V_{dc} because the DC-link voltage is the sum of the two capacitor voltages,

By Eq. 9 and Eq. 13, the neutral point current which flows to the neutral point is calculated as

$$i_n = 2\sqrt{V_{out} I_{out} C\omega} \cos\left(\omega t - \frac{\pi}{4}\right) \qquad (14).$$

By controlling the neutral point current, the capacitor voltages are oscillated according to Eq. 5–6 to absorb the power ripple.

Figure 4 shows the absolute current reference relationship between the output current and the neutral point current. When the single-phase T-type NPC inverter employs CCM as in the conventional method [15], the neutral point current control and the output current control interrupt with each other during the period where the command value relationship is $|i_n^*|>|i_{out}^*|$ as shown in the shaded period in Fig. 4. When the neutral point current flows during the period, the current which is larger than the output current reference value, flows to the grid-tied inductor. Thus, the output current is affected by the neutral point current. In the conventional method, only the output current is controlled in the period in order to avoid the interference. Consequently, the power ripple still exists in the DC-link since the neutral point current is different from the reference value.

Therefore, DCM is applied for the current controls of the single-phase T-type NPC inverter drawn in Fig. 2 in order to avoid the interference. In DCM, there are zero-current intervals, where the inductor current becomes zero and all switching devices are turned off. For this reason, the interference of the two current control is eliminated by flowing each current during the zero-current interval of the other current. In particular, the neutral point current flows during the zero-current interval of the grid current and vice versa. If the zero-current interval of each current is designed to be long enough to flow the other current, two currents can be independently controlled simultaneously.

Figures 5 and 6 show the current waveform of the neutral point current and the output current of the T-type NPC inverter drawn in Fig. 2 with DCM. As shown in Fig. 5, the zero-current interval is produced after flowing the neutral point current i_n.

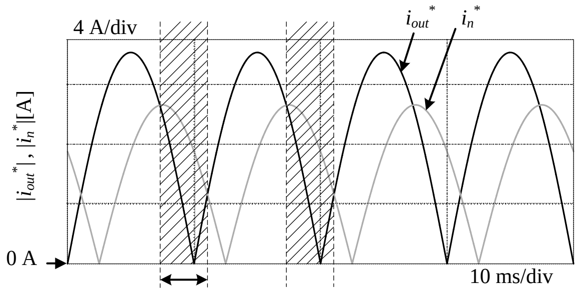

Fig. 4. The relationship of the absolute current reference value between the output current and neutral point current. The neutral point current control and the output current control interrupt each other in CCM during the shaded area in Fig. 4.

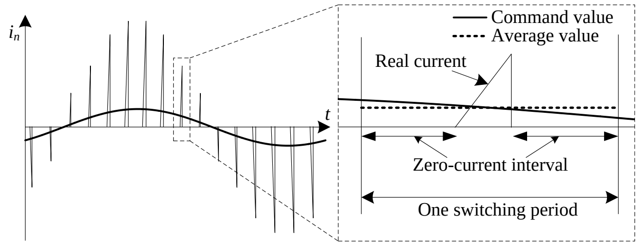

Fig. 5. Waveform of i_n operated in the DCM

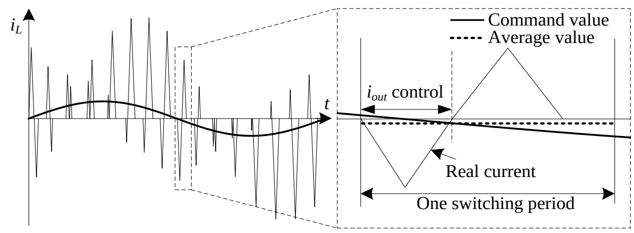

Fig. 6. Waveform of i_L operated in the DCM

By the control of this neutral point current according to Eq. 14, the two capacitor voltages oscillate according to Eq. 5–6, achieving the power decoupling control. As shown in Fig. 6, the inductor current i_L flows during the zero-current interval of the neutral point current so that the sum of i_L and i_n results in the sinusoidal output current. Thus, two currents are simultaneously controlled using only one of connected inductors in series, leading to the achievement of the power decoupling control and the sinusoidal output current control simultaneously.

IV. Switching Pettern Selection for Inductor Current Reduction

In the proposed method, there are two switching patterns to achieve the operation. In this chapter, the features of each switching pattern, and the selection method of the suitable switching pattern, are explained. Note that the current reference values are assumed to be "i_{out}^* = +, i_n^* = –" in this chapter.

Fig. 7 and 8 show the example switching patterns. The output current is controlled by the switching pattern in Fig. 7. Thw neutral point current is controlled by the switching patterns in Fig. 8. Note that the neutral point current flows to the inductor i.e. output side. The neutral point current interrupts the output current control. Therefore, interruption is compensated by the output current control. Fig. 9 shows the general form of the inductor current. At first, the output current is controlled by using the pattern which shown in Fig. 7. After that, the neutral point current is controlled using the zero-current period of i_{out} control. However, as shown in Fig.8, there are two of switching patterns to achieve the operation. Output current and neutral point current does not change even which switching pattern is selected. However, the peak value and the RMS value of the inductor current are different. Hence, the inductor current is suppressed by selecting the optimal switching pattern. In this paper, the two of current control method are called "1st method" and "2nd method".

"1st method": the switching pattern that the polarity of capacitor voltage and output voltage becomes same, is selected.

"2nd method": the switching pattern that the polarity of the neutral point through inductor, becomes same as the polarity of the output current, is selected.

As the feature of the 2nd method, the inductor current is reduced compared to the 1st method. The compensation value of the output current becomes minimum because the polarity of the neutral point current is same as the output current As shown in Fig. 9. However, the 2nd method cannot be used when the capacitor voltage is lower than the output voltage because the polarity of capacitor voltage and the output voltage is opposite.

On the contrary, the 1st method achieves the current control at all time because the polarity of the capacitor voltage and output voltage are same. However, the polarity of neutral point current through inductor is opposite to the polarity of the output current. Thus, higher compensation value of the output current is required in order to eliminate the interruption due to the neutral point current control.

Consequently, the inductor current is suppressed as the minimum value by applying 2nd method during the period that 2nd method is applicable.

V. Simulation Result

Table I shows the simulation parameters. Fig. 10 shows the harmonic analysis of the input current, whereas Fig. 11(a) and (b) show the waveforms of the input current, the capacitor voltages, the output voltage, the inductor current without and with the proposed power decoupling control respectively.

As shown in Fig. 11(a), the input current oscillates at twice the grid frequency because the use of the small capacitance of C leads to the high current ripple on DC-link according to Eq. 3. On the other hand, as shown in Fig. 11(b), the current ripple of the input current is reduced significantly compared to that in Fig. 11(a) because the capacitor voltages V_{C1} and V_{C2} oscillate to absorb the power ripple in the proposed power decoupling method. In addition, by the proposed method, the component of 100 Hz, i.e., twice the grid frequency is reduced by 97.1%

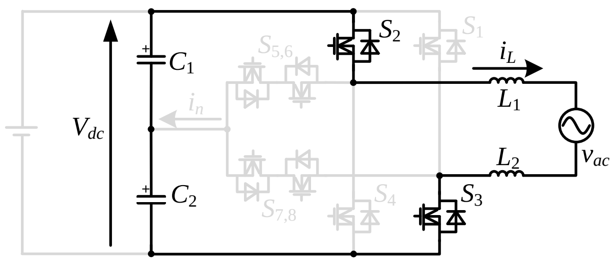

Fig. 7. The switching pattern to control the output current as positive polarity.

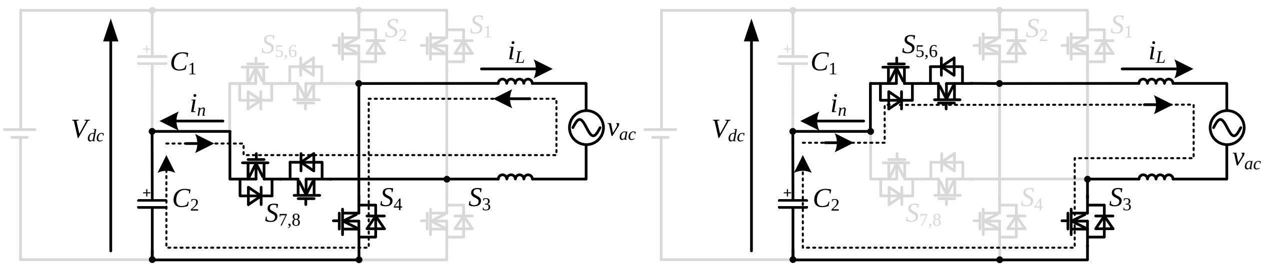

(a). inductor current increases (b).inductor current decreases

Fig. 8 The switching pattern to control the neutral point current as negative polarity. The polarity of neutral point current becomes same even which pattern is selected. However, the polarity of inductor current is different.

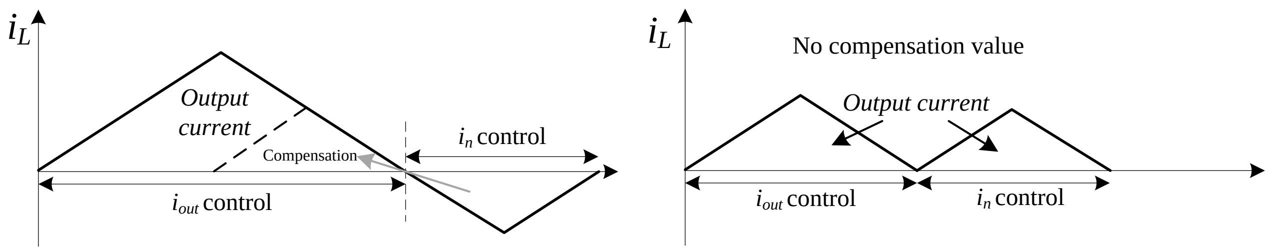

(a). small inductor current due to 2nd method (b).large inductor current due to 1st method

Fig. 9. The inductor current waveforms. The output current and neutral point current become same, whereas the RMS and peak value of the inductor current is different.

compared to that result without the power decoupling method whereas the THD of the output current is 1.31%.

Figure 12 shows the inductor current waveforms when the output power is 500 W. As the current control method, only the 1st method is employed in Fig. 12(a), whereas both the 1st and the 2nd method employed in Fig. 12 (b). The RMS value of i_L shown in Fig. 12 (b) is 19.0 A whereas Fig. 12 (b) is 38.8 A regardless the common output current and the neutral point current. Thus, the RMS inductor current of Fig. 12 (b) is reduced by 50.0% compared to the result of Fig. 12 (a) whereas the operation capability does not change.

VI. Experimental Result

Table II shows the experimental parameters. The experiments have been done with an open-loop. In general, percent impedance $\%Z_L$ of the grid-tied inductor is designed around 5%. However, as shown in Table II, the grid-tied inductor of the prototype is 45μH (series connection of the two inductors 22.5 μH). Hence, the $\%Z_L$ is 0.16%. Furthermore, the additional inductor which is required for conventional power decoupling control is not needed.

Figure 13 shows the harmonic analysis of the input current, whereas Figs. 14 (a) and (b) show the waveforms of the output voltage, the output current, inductor current, and the input current with and without the proposed power decoupling method at a 500 W load respectively. From Fig. 14 (b), the form of the inductor current is same as the ideal inductor current as shown in Fig. 12(b). In addition, the output voltage is controlled in the sinusoidal waveform at 50 Hz whereas the input current is compensated by the proposed method. The THD of the output current is 1.9%. Furthermore, in Fig. 13, by using the proposed method, the component of 100 Hz, i.e., twice the grid frequency is reduced by 67.7% compared to that result without the power decoupling control.

VII. Conclusion

This paper proposed the power decoupling method based on DCM for T-type NPC inverter without any additional passive components and switching devices. The proposed control method achieved the low ripple current at the DC-link and the low grid current THD. Thus, the reduction of the system size due to DCM, and the long lifetime are expected from the active power decoupling method. As the simulation result, the current ripple of the input current at twice the grid frequency is reduced by 90.2%. Moreover, the output current THD is 1.87%.

TABLE I Simulation Parameters

Parameter	Symbol	Value
Output power	P_{out}	500 W
Output voltage	v_{ac}	100 V
Output frequency	f_{out}	50 Hz
DC link voltage	V_{dc}	400 V
Capacitor	C_1,C_2	120 μF
Inductor	L_1,L_2	22.5 μH

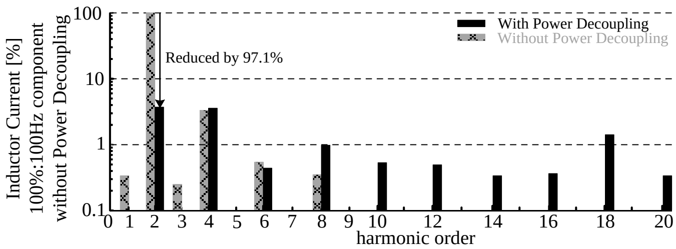

Fig.10. Harmonic components of input current

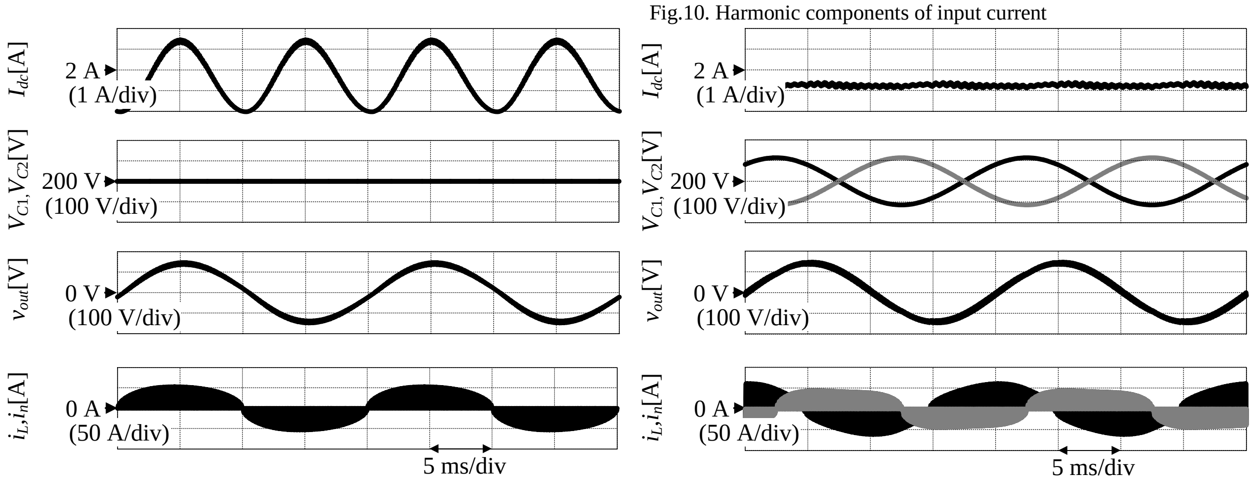

(a) Operation without power decoupling control.
(b) Operation with power decoupling control.

Fig. 11. Waveforms of input current, capacitor voltages, output voltage and output current.in steady state.

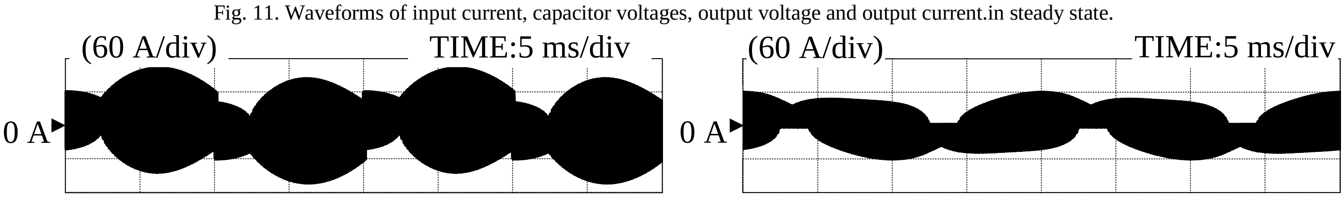

(a)only 1st method is applied
(b)1st and 2nd method is applied

Fig. 12. Inductor current waveform operated in DCM.

TABLE II INVERTER PARAMETERS

Parameter	Symbol	Value
Output power	P_{out}	500 W
Output voltage	v_{ac}	100 V
Output frequency	f_{out}	50 Hz
DC link voltage	V_{dc}	400 V
Capacitor	C_1,C_2	166 μF
Inductor	L_1,L_2	22.5 μH

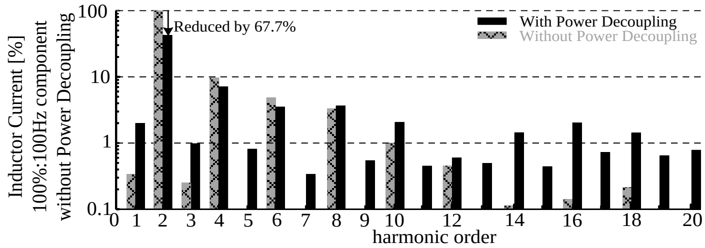

Fig.13 Harmonic components of input current

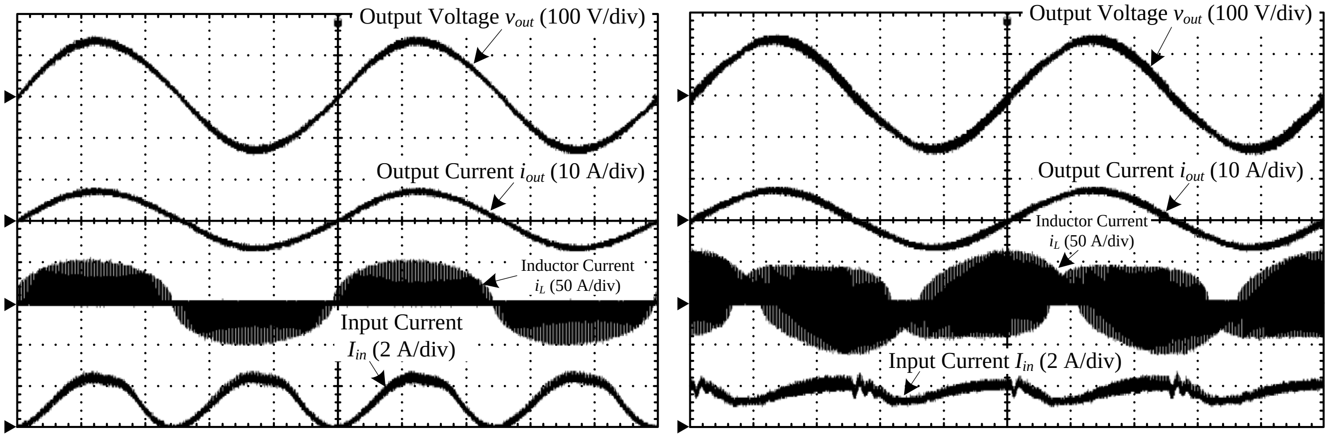

(a) Operation without power decoupling control. (b) Operation with power decoupling control.

Fig. 14. Waveforms of input current, output voltage, output current and inductor current in steady state.

In the proposed method, there are two switching patterns to achieve the active power decoupling control. However, the inductor current is different between the two switching patterns. Thus, the RMS value of the inductor is suppressed by selecting the suitable switching patterns.

As the experimental result, the output current is controlled as 50 Hz sinusoidal waveform whereas the current ripple of the input current is suppressed compared to that without power decoupling control. Furthermore, the form of the inductor current is same as the ideal current as shown in Fig. 12(b) to suppress the inductor current. As a result, the second harmonics component of the input current is reduced by 67.7% compared to that result without the power decoupling control whereas the output current THD is 1.9%.

In the future work, operation at a rated load of 1 kW with a critical current mode, and loss analysis with both simulation and experiment will be considered in order to clarify the accurate efficiency.

REFERENCES

[1] F. Jamadi, M. Arabpour, M. Abdolzadeh, "Performance Comparison of Parabolic and Flat Plate Solar Collectors Utilizing in the Heating System of a Room-An Experimental Investigation", *IJRER* Vol.7, No.4, (2017)

[2] E. Duque, P. Ortiz-Grisales, A. Isaza, A. Luján, S. Chica and J.D. González-Ruíz, "Design and Construction of a Stand-Alone PV System for Charging Mobile Devices in Urban Landscapes in Medellin", *IJRER* Vol.8, No.1, (2018)

[3] A. Boumaiza, S. Abbar, N. Mohandes, A. Sanfilippo, "Modeling the Impact of Innovation Diffusion on Solar PV Adoption in City Neighborhoods", *IJRER* Vol.8, No.3, (2018)

[4] S. Kirmani, M. Jamil, I. Akhtar, "Effective low cost Grid-Connected Solar Photovoltaic System to Electrify the Small Scale industry/Commercial Building", *IJRER* Vol.7, No.2, (2017)

[5] E. Kabalci, Y. Kabalci, R. Canbaz, G. Gokkus, "Single Phase Multilevel String Inverter for Solar Applications", *ICRERA2015*, pp. 109-114,(2015)

[6] A. Jamatia, V. Gautam, and P. Sensarma, "Power decoupling method for single phase PV system using Ćuk derived micro-inverter", *IEEE ECCE2016 Conf.*, EC-0529, (2016)

[7] D. Vinnikov, R. Kosenko, A. Chub, and E, Liivik, "Shade-tolerant photovoltaic microinverter with time adaptive seamless P-V curve sweep MPPT", *IEEE EPE2017 Conf*., 0648, (2017)

[8] N. Ramzan, Z. J. Khan, P. Naseer, A. Akbar, and N. Zaffar, "Grid tied solar micro-converter with optimizer-mode operation for weak-grid operation", *IEEE APEC2017 Conf.*, pp.2068–2075, (2017)

[9] N. Pragallapati, T. Lodh, V. Agarwal, "Parallel-Input Series-Output Interleaved Flyback based Solar PV Module Integrated Micro-Inverter", *ICRERA2015*, pp. 716-720, (2015)

[10] K. M. Sundaram, P.Anandhraj, V.V. Ambeth, "Photo-Voltaic Array Fed Transformer-less Inverter with Energy Storage System for Non-isolated Micro Inverter Applications", *IJRER* Vol.7, No.1, (2017)

[11] K. Abe, H. Haga, K. Ohishi, and Y. Yokokura,"Current Ripple Suppression Control Based on Prediction of Resonance Cancellation Voltage for Electrolytic-Capacitor-Less Inverter",*IEEJ J. Industry Applications*, vol.6, no.1, pp.1-11, (2017)

[12] H. Hu, S. Harb, N. Kutkut, I. Batarseh, Z. J. Shen : "Power Decoupling Techniques for Micro-inverters in PV Systems — a Review," *Energy Conversion Congress and Exposition 2010*, pp.3235-3240, (2010)

[13] K. H. Chao, P. T. Cheng: "Power Decoupling Methods for single-phase three-poles AC/DC converters", *Energy Conversion Congress and Exposition 2009*, pp. 3742-3747 (2009)

[14] [13] S.Yamaguchi, T.Shimizu: "Single-phase Power Conditioner with a Buck-boost-type Power Decoupling Circuit", *IEEJ Journal of Industry Applications*, Vol. 5, No. 3, pp. 191-198 (2016)

[15] M. Abe, H. Haga, S. Kondo, "Electrolytic capacitor-less single-phase AC/DC converter using T-type NPC circuit", *IEEE INTELEC2015 Conf.*, 2015, (2015)